Modern Physics Letters B, Vol. 7, No. 21 (1993) 1343–1364

THEORETICAL AND EXPERIMENTAL STUDIES ON SILOXENE

P. DEÁK
Physical Institute of the Technical University of Budapest, Budafoki út 8., H-1111 Budapest, Hungary

M. STUTZMANN, M. S. BRANDT, M. ROSENBAUER, S. FINKBEINER, H. D. FUCHS, and J. WEBER
Max-Planck-Institut für Festkörperforschung, Heisenberg Str. 1, D-7000 Stuttgart 80, Germany

Received 12 April 1993

Structural and optical properties of siloxene ($Si_6O_3H_6$) and its derivatives obtained by chemical substitution or annealing are reviewed. The preparation of siloxene is briefly described and results of x-ray diffraction and infrared absorption are shown. The equilibrium structures of stoichiometric siloxene and the electronic properties of the corresponding 2, 1, and 0-dimensional Si-clusters are obtained from quantum chemical calculations and compared to other calculations. Experimental results concerning luminescence, luminescence excitation, absorption coefficients, magnetic resonance, and stability are presented. The origin of the optical properties of siloxene is discussed based on the accumulated experimental data and on the results of theoretical modeling.

1. Introduction

Integrated optoelectronic devices based on standard silicon technology is a much desired goal of modern semiconductor physics. Heteroepitaxy of GaAs on Si, Si-based ternary alloys, strained layer Si–Ge superlattices and, more recently, anodically etched porous silicon are among the promising approaches. The luminescence of porous Si[1,2] has caused great excitement in the past two years; however, a detailed microscopic understanding of its optical properties is still missing. Most groups favor the quantum confinement approach, which explains the observation of strong optical transitions in porous silicon as a quantum size effect: carriers are confined in small Si "quantum-wires" or nanocrystals, produced somehow during anodic oxidation with a sufficiently narrow distribution of sizes and shapes. Other researchers have invoked specific substances such as hydrogenated amorphous silicon, hydrogenated Si-surfaces, or polysilanes in order to explain the particular properties of porous Si. Based on the comparison of many structural and optical characteristics, our group has proposed that certain derivatives of siloxene ($Si_6O_3H_6$) are the origin of the photo-luminescence detected in porous Si.[3,4]

Arguments supporting[5,6] or rejecting[7,8] this assignment have been reported, but irrespective of their role in porous Si, siloxene and structurally related substances are interesting materials on their own. The luminescence observed in as-prepared siloxene is, together with the photoluminescence obtained from porous Si, probably the most efficient radiative recombination process reported for Si-related materials at room temperature. As demonstrated in Fig. 1, the external quantum efficiency for siloxene luminescence at 300 K is at least two or three orders of magnitude higher

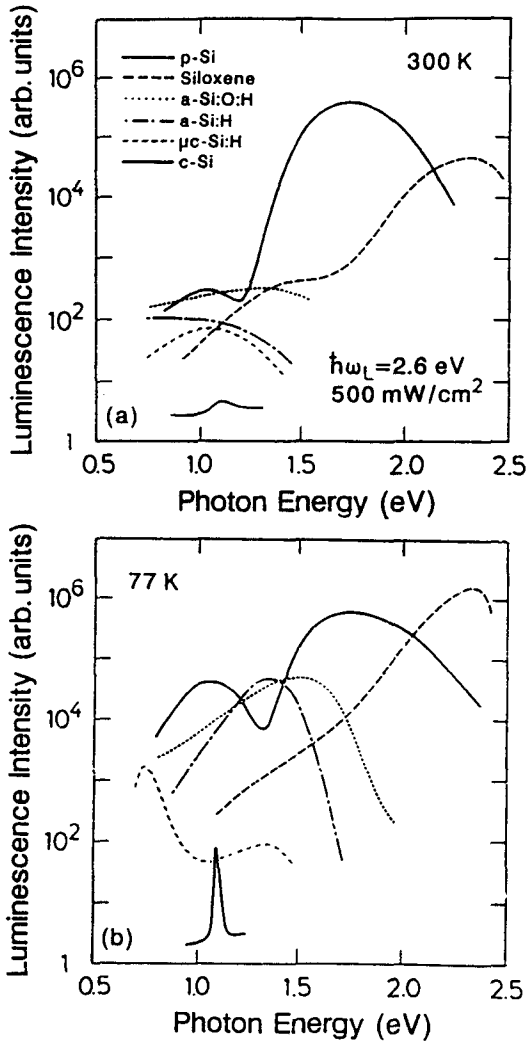

Fig. 1. Comparison of the luminescence from porous Si, Wöhler siloxene, amorphous hydrogenated Si and Si–O alloys, microcrystalline silicon and crystalline Si. Note the logarithmic intensity scale. Upper figure: $T = 300$ K, lower figure: $T = 77$ K.

than typical luminescence efficiencies observed for other Si-networks (crystalline Si, microcrystalline Si, amorphous Si, or disordered Si:O:H alloys). It increases by at least another order of magnitude upon cooling to 77 K. Although discovered and first described more than a century ago by Wöhler,[9] the electronic and optical properties of siloxene and its derivatives remain largely unexplored. Very few reports about siloxene can be found in the literature and most of them date back before 1970. The purpose of this paper is to present an overview of the interesting aspects of siloxene, based mainly on the experimental and theoretical work of our group. The general question we pose is: "What is the origin of the bright luminescence in siloxene derivatives?"

2. Preparation of Siloxene

Siloxene can be prepared by chemical transformation of $CaSi_2$. $CaSi_2$ is a layered silicide consisting of alternating Si and Ca planes.[10] For preparation of siloxene, the Ca-layers are removed by a topochemical reaction at low temperature and the remaining isolated Si-planes are stabilized by intercalation of H and OH bond terminators (Fig. 2). The original recipe for this reaction was given by Wöhler[9] and consists simply of placing $CaSi_2$ into concentrated aqueous HCl at 0° C for several hours. The resulting *Wöhler siloxene* is a bright yellow substance with a strong room-temperature luminescence in the green ($\approx$ 550 nm). Wöhler siloxene is stable for months under normal ambient conditions, but photooxidizes under UV illumination. A more careful preparation method for stoichiometric siloxene has been described by Kautsky.[11] Instead of using aqueous HCl, Kautsky has prepared

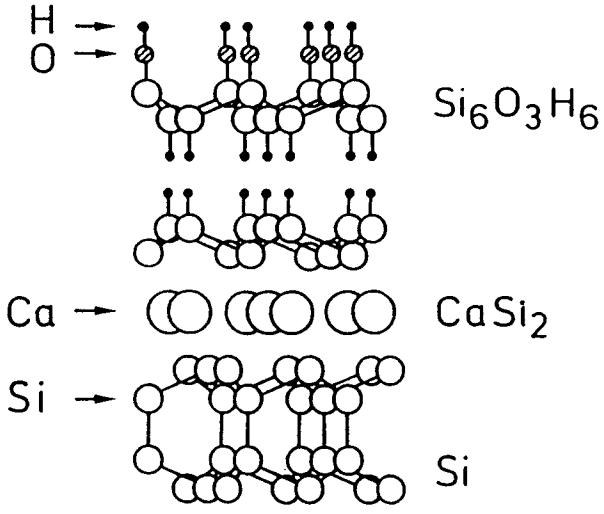

Fig. 2. Comparison of the structure of crystalline Si, $CaSi_2$, and siloxene ($Si_6O_3H_6$) in the Si-plane modification.

siloxene with a mixture of HCl, water, and ethanol, again at 0° C, but under exclusion of air and light. *Kautsky siloxene* is a whitish-gray substance that is very reactive and sensitive to UV light. It shows a blue photoluminescence ($\approx$ 500 nm) under UV excitation. According to Kautsky, the yellow Wöhler-siloxene consists of a mixture of stoichiometric siloxene with derivatives in various stages of oxidation. An interesting aspect for the growth of siloxene on crystalline silicon is shown in Fig. 2: since the Si–Si distances in both $CaSi_2$ and siloxene (planar modification) agree with those of bulk crystalline Si to within better than 0.5%,[12] it should be possible to grow siloxene epitaxially on Si(111) substrates. To this end, one first grows a thin epitaxial $CaSi_2$ layer,[10] which is then transformed into siloxene by the topochemical reaction described above. First attempts to use this method for the preparation of thin luminescing siloxene layers on crystalline Si are very promising.[13]

3. Structural Properties of Siloxene

Siloxene belongs to the large class of silicon-based polymers or "silicon-backbone-materials" that are characterized by the fact that each silicon atom has, in contrast to bulk crystalline or amorphous Si, less than four silicon nearest neighbors.[14] The preparation of these materials occurs under conditions that are very different from those of crystalline Si growth or amorphous Si thin film deposition, so that investigations on these materials have basically remained within the domain of organosilicon chemistry. In the specific case of siloxene, the important chemical ingredients in addition to silicon are oxygen and hydrogen. Oxygen serves, as usual in organosilicon chemistry, as a link between two silicon atoms, allowing polymerization of the Si-clusters to macroscopic structures, whereas hydrogen serves as an efficient bond terminator that prevents the whole network from having unacceptably high defect densities. The spelling siloxene does not refer to double bonds in the structure. Rather, it serves as a distinction from polysiloxanes, in which there are no Si–Si bonds at all.

In Figs. 3(a) to (c), we show three possible crystalline modifications of stoichiometric siloxene with the same sum formula, $[Si_6O_3H_6]_n$. The three modifications are characterized by a decreasing dimensionality of the Si-backbone structure. Figure 3(a) shows the Si-*plane* configuration, in which the Si atoms form a quasi-two-dimensional structure very similar to the (111) planes of bulk crystalline Si. Each silicon atom is bonded to three other Si-atoms, and the remaining unbonded sp^3-hybrid is saturated by OH and H radicals in such a way that ideally one side of the plane is terminated by H, and the other side by OH-groups. The Si planes are then stacked upon each other to form a three-dimensional crystal similar to graphite. The inter-plane bonding is provided by much smaller dipole forces. It is found both theoretically and experimentally that the Si-plane structure in Fig. 3(a) can lower its energy by allowing the oxygen atoms to be inserted into the Si-plane. This oxidation of the silicon backbone can occur in two ordered ways. In Fig. 3(b) the oxygen atoms have been inserted in such a way as to isolate quasi-one-dimensional

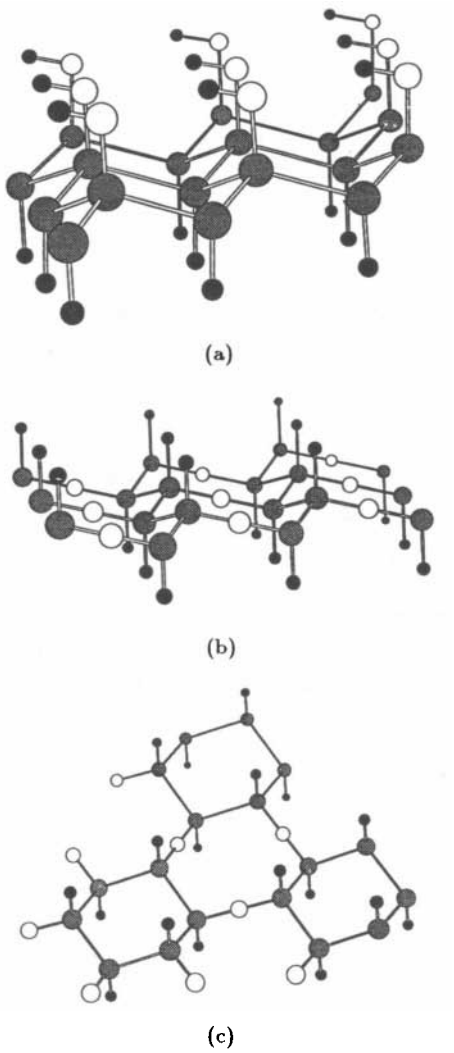

Fig. 3. Equilibrium of different modifications of stoichiometric siloxene, $Si_6O_3H_6$: (a) Si planes, (b) Si chains, (c) sixfold Si rings. Shaded spheres symbolize Si, small dark spheres hydrogen, and light spheres oxygen.

silicon *chains*, whereas in the case of Fig. 3(c), quasi-zero-dimensional Si_6-*rings* are formed. In Figs. 3(b) and (c), thus, one has the same planar bonding structure as in the case of Fig. 3(a), however, with a lower dimensionality of the Si-backbone. Note that in the ideal case all three modifications can be entirely free of structural defects provided that the hydrogen and oxygen contents are as required by stoichiometry.

The structure originally proposed by Kautsky for ideal siloxene is the ring-modification shown in Fig. 3(c).[15] His claim is based mainly on chemical substitution studies in which the hydrogen terminators have been replaced by halogen

atoms, amino, or hydroxyl groups.[16] Also, he has found siloxene to form small hexagonal crystallites (although no crystalline diffraction patterns could be found in X-ray diffractometry). Based on this evidence, Kautsky ruled out the suggestion of Wiberg[15] about the chain modification. Later, further refining the preparation technique of Kautsky, Weiss *et al.*[12] have achieved single crystalline flakes of siloxene, and characterized them by X-ray diffraction. Their analysis, later confirmed by Ubara *et al.*,[17] led to the plane-modification shown in Fig. 3(a). The Si–Si bonding distance within the planes has been found to be almost identical to that of bulk crystalline Si, while the spacing between adjacent Si-planes was ≈ 6.3 Å.

How can the structure of the plane-modification be reconciled with the results of chemical substitution studies? Theoretical calculations (see next section) predict that the plane-modification is metastable against insertion of oxygen atoms from the Si–O–H bonds into the Si–Si backbone (forming Si–O–Si bonds). The insertion does not occur in a sufficiently ordered fashion to produce the structures shown in Figs. 3(b) and (c) selectively. Instead, upon exposure to higher temperature or oxidizing environment, a random mixture of all three phases is likely to result, and the X-ray diffraction pattern gets lost (n.b. the X-ray experiments of Weiss *et al.* and Ubara *et al.* have been carried out *in situ* on as-prepared samples). The calculations predict the ring-modification slightly more favorable in energy than the chain-modification, therefore, a dominance of rings over long chains is expected.

The upper trace of Fig. 4 shows a powder diffraction pattern for a sample of as-prepared siloxene (with some silicon-crystallite content) that clearly exhibits a peak

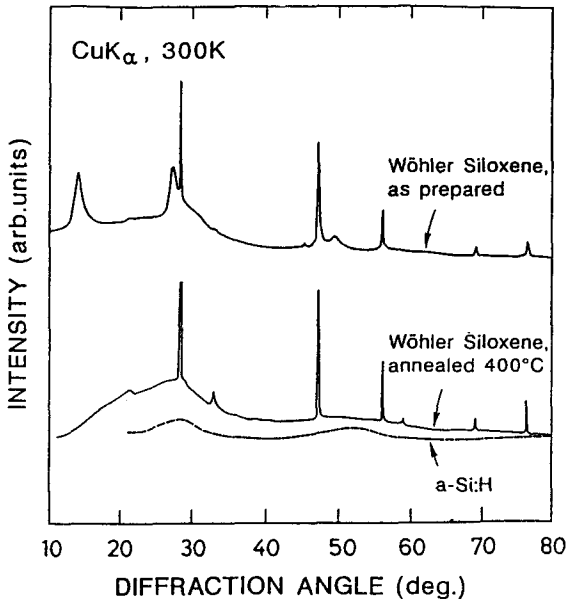

Fig. 4. X-ray diffraction spectra of as-prepared Wöhler siloxene and after annealing at 400° C. The spectrum of amorphous silicon is shown for comparison (dashed curve).

at a diffraction angle ($\approx 14°$) corresponding to the expected interlayer-spacing of 6.3 Å. (In addition, the same sample shows further peaks coinciding with or close to the powder diffraction pattern of randomly oriented Si crystals). Annealing of the sample at 400° C causes a complete disappearance of the peak related to the Si-plane structure in Fig. 3(a), leaving only a broad background similar to the diffraction spectrum of amorphous silicon (lower two traces in Fig. 4). The disappearance of the peak characteristic to the regular planar spacing can also be a consequence of the condensation of the planes through the formation of random Si–O–Si linkages between them.[12] That this is not the only thing happening, is demonstrated by infrared spectroscopy.

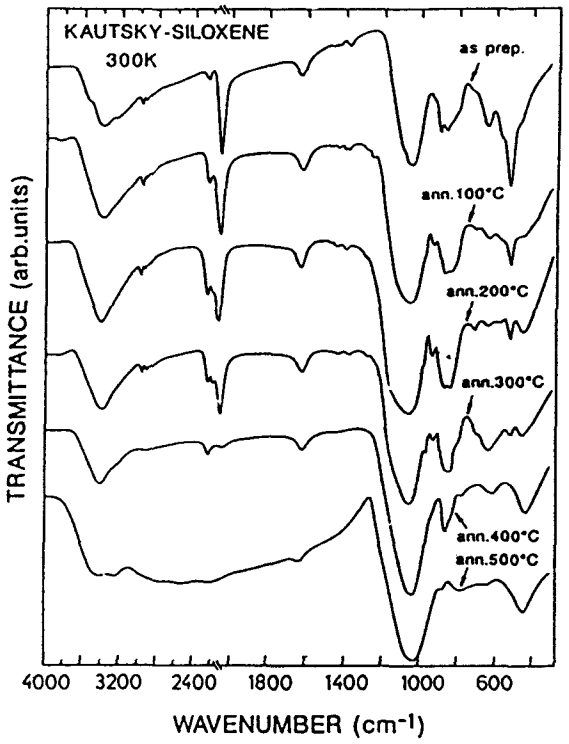

Fig. 5. Room-temperature infrared transmittance of Kautsky siloxene as-prepared (upper trace), and annealed at various temperatures.

Infrared absorption spectra of as-prepared siloxene are shown in the upper trace of Fig. 5. One clearly observes the well-known Si–H–related vibrational modes around 600–900 and 2100 cm^{-1}, the OH–related bands at 1600 and 3400 cm^{-1}, and the Si–O–Si stretching vibrations at around 1100 cm^{-1}. Characteristic for as-prepared siloxene are a sharp hydrogen stretch mode at 2100 cm^{-1} and a Si-

related mode at 520 cm^{-1} of similar width. We have previously assigned this line to a phonon mode of the two-dimensional Si planes.[4] Upon annealing, the sharp 520 cm^{-1} Si-mode is quickly destroyed, as oxygen is inserted into the planes.

Raman scattering experiments corroborate the gradual breaking up of the Si-planes into smaller fragments.[4,15] As-prepared siloxene shows a sharp peak at 515 cm^{-1} (which we assign to the phonon mode in the Si-planes of siloxene in the plane-modification). Upon low temperature annealing, a second, a peak around 480 cm^{-1} appears. This broad structure can be assigned to small planar fragments of silicon. Upon increasing the annealing temperature both bands disappear into a broad peak around 460 cm^{-1} that is also observed in the infrared absorption spectrum.

4. Theoretical Modeling of Siloxene

Since no theoretical studies of siloxene have been published earlier, we have performed a number of calculations concerning electronic, structural, and vibrational properties of single planes of the three ideal siloxene modifications shown in Fig. 3. In fact, the structures in this figure are the results of our total energy minimization.[18] We have modeled the plane-($[HSi_2(OH)]_{3n}$), chain-($[(HSi_2H)O]_{3n}$) and ring-($[(SiH)_6O_3]_n$) modifications of siloxene by cyclic clusters containing $n = 3$ or $n = 4$ units. Details of the cyclic cluster model are given elsewhere.[19,20] It assumes the Born–von Kármán boundary conditions to be fulfilled for the cluster itself, without prescribing the Bloch condition (i.e., microscopic periodicity). The cyclic boundary conditions ensure the full point group symmetry of the crystal, but the only allowed translations are the unit vectors defining the cluster. Consequently, the only wave vector is $\mathbf{K} = 0$, i.e., the calculation can be performed entirely in direct space. However, since $n > 1$, the $\mathbf{K} = 0$ point represents a sampling of wave vectors from the primitive Brillouin zone (BZ) of the two-dimensional hexagonal crystal. For $n = 3$, the cyclic clusters of the plane- and chain-modifications contain 9 unit cells. Accordingly, the calculation takes the center ($\bar{\Gamma}$), the two corner points ($\bar{K}$) and six other points ($\bar{\Sigma}$) between $\bar{\Gamma}$ and the midpoints of the border lines ($\bar{M}$) of the primitive BZ into account (see Fig. 6). Note, that the BZ of the chain-modification is a slightly irregular hexagon and the $\bar{M}$ points (and consequently the $\bar{\Sigma}$ points) along chain directions are not equivalent with the ones along the links between chains. In the case of the ring modification, a cyclic cluster with $n = 3$ contains only 3 units, and the represented primitive wave vectors are only $\bar{\Gamma}$ and the two $\bar{K}$, while a calculation with $n = 4$ represents $\bar{\Gamma}$ and three $\bar{M}$ points. The deviation in one-electron eigenvalues at $\bar{\Gamma}$ is smaller than 0.1 eV in the two calculations, indicating that the average electron density is about equally well-represented by both sets. The difference between the cyclic cluster model and the usual supercell bandstructure calculations utilizing special wave vector summations lies mainly in the fact, that the physical size of the "crystal" is limited to that of the actual cyclic cluster. Since small angle X-ray scattering[21] on our siloxene samples show a

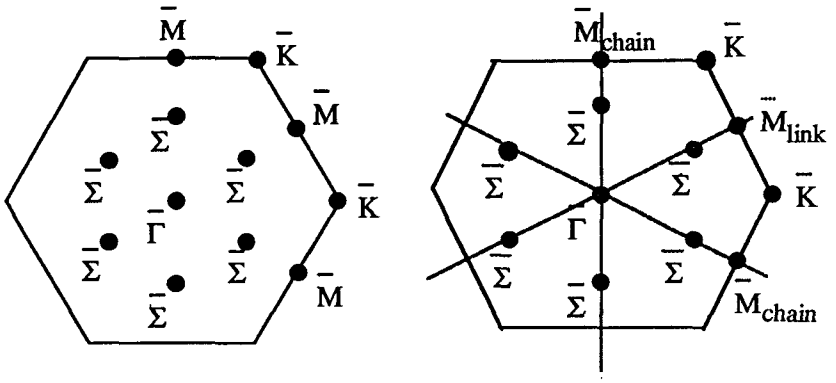

Fig. 6. The two-dimensional Brillouin zones of (a) the plane-, ring- and (b) the chain-modification of siloxene, showing the wave vectors taken into account in the cyclic cluster calculation (see text).

crystallite size of $\approx$ 20 Å, the cyclic clusters considered here are in the same size range where "ideal" structures of the three modifications can be expected.

We have employed various semi-empirical methods to calculate the equilibrium geometry, relative stability, electronic transitions and vibrational frequencies of the above structures. Since the long-range order in the experimentally studied siloxene samples are also strongly limited, the application of these basically chemical methods is certainly justified here. (The properties of crystalline silicon and α-quartz could also be reproduced to reasonable accuracy[20,22]). Among the various semi-empirical methods MINDO/3 (modified intermediate neglect of differential overlap) has been found to give the most reliable geometry in silicon based systems.[20,23] Since MINDO/3 is known to underestimate the strength of Si–Si and overestimate the strength of Si–O bonds, we have performed calculations also by using the AM1 (Austin Model) method that is more reliable in predicting bond strengths and force constants. Since none of the above methods are suitable to describe the conduction band of c-Si, the electronic transitions have been calculated by using the spectroscopic version of the complete neglect of differential overlap method, CNDO/S. We have employed the parametrization determined for saturated molecules (including Si 3*d* orbitals into the basis) to calculate one-electron eigenvalues end eigenfunctions at the equilibrium geometry supplied by MINDO/3. The electronic transitions have been obtained from a CI (configuration interaction) calculation over the lowest 120 singly excited configurations. (For references about semi-empirical methods see Ref. 20).

The MINDO/3 and AM1 methods result in essentially identical geometry in the case of all three structures (shown in Fig. 3). The nearest neighbor Si–Si distances are within 0.01 Å the same as the one calculated for bulk silicon. The heat of formation for the plane modification is −2.85 eV/unit in AM1. In establishing the relative stability of the three structures, one has to be aware of the fact that the

accuracy of total energies calculated by semi-empirical methods can only be the same if the systems contain roughly the same number from each of the different bonds. The energy change upon the transformation of the plane-modification into either the chain- or the ring-modification arises from changing the number of bonds (1 Si–Si and 1 O–H bond is broken, and 1 Si–O and 1 Si–H bond is created for every pair of silicon atoms) and from the subsequent relaxation of the electrons and nuclei. Even relatively small errors in the individual binding energies may accumulate to a substantial amount in such a case. The errors in the individual binding energies can be estimated comparing calculated and experimental bond dissociation energies of appropriate molecules. Taking these into account, the energy gain upon the transformations: plane → chain and chain → ring can be estimated to be 0.26 and 0.62 eV/Si-pair, respectively, by AM1.

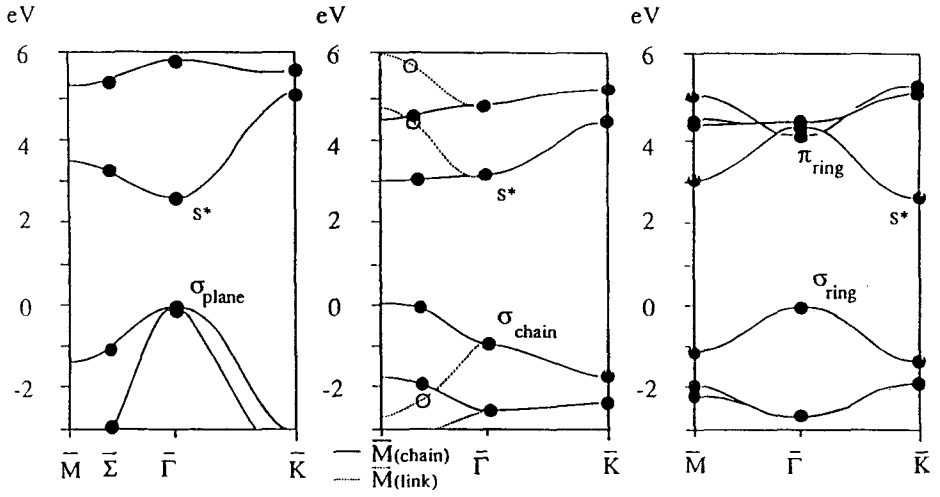

Fig. 7. Calculated band structure of siloxene in the plane, chain, and ring modification. See text for details.

Figure 7 summarizes our results for the electronic band structure of the plane-, chain-, and ring-modifications of siloxene. The cyclic cluster calculations result in one-electron eigenvalues at the discrete wave vectors sampled in $\mathbf{K} = 0$. These calculated values are represented by dots while the "bands" are graphically interpolated (using simple symmetry and compatibility relations) in order to facilitate evaluation. The conduction band states are shown as separated from the valence band states by the lowest calculated (direct) transition energy involving the given states. Contrary to the indirect band structure of bulk silicon, the two-dimensional Si backbone in the plane-modification gives rise to a direct bandgap of ≈ 2.7 eV at the center of the BZ. The top of the valence band (VB) is a bonding combination

(σ_{plane}) of Si $3p_x$ and $3p_y$ orbitals along the plane with negligible coefficients on oxygens or hydrogens. The bottom of the conduction band (CB) is an antibonding state (s^*) of predominantly Si $3s$ character, also confined to the quasi-two-dimensional Si network. In the chain-modification a somewhat larger direct gap of $\approx 3.0\,\text{eV}$ is obtained at a wave vector parallel to the Si chains. The top of the VB (σ_{chain}) is a bonding combination of Si $3p_x$ orbitals along chain directions. Two neighboring chains are antibonded, with the bridging O atoms in a nodal plane. So, the electrons in these orbitals are confined to the quasi-one-dimensional Si-chains. The Si–O–Si bridges between the chains give rise to a much larger splitting between bonding and antibonding states (dotted lines in Fig. 7b) and in effect act as an electronic barrier between the chains that can thus be regarded as "quantum wires". Indeed, the electronic structure of the chain-modification of siloxene is quite similar to that of a crystalline array of linear polysilane chains.[24] The band structure of siloxene in the Si_6-ring modification is shown in Fig. 7(c). In this modification the direct gap is again larger than in the other two: it is $\approx 3.5\,\text{eV}$ at $\bar{K}$. The lowest direct transition at $\bar{\Gamma}$ has an energy of $\approx 4.2\,\text{eV}$. The lowest indirect transition between $\bar{\Gamma}$ and $\bar{K}$ is $\approx 2.8\,\text{eV}$.

It is interesting to look more closely at the electronic properties of siloxene in the ring-modification, since in the relevant chemical literature the existence of such rings has been invoked in order to explain the remarkable color and luminescence of certain siloxene derivatives.[16,25,26] Figure 8 shows a contour plot of the probability distribution of an electron at the top of the valence band of stoichiometric siloxene in the ring-modification. This orbital consist of Si $3p_x$–$3p_y$ hybrids in σ-bonded combination around the rings. The positions of Si-atoms coincide with the valleys in the ring structure. The two narrow peaks in the center of Fig. 8 are due to the oxygen $2p$ orbitals. Note that there is no electron density on either side of the oxygen connecting the two Si_6-rings. The Si–O–Si antibond between rings confines the electron mainly on the rings, giving rise to a molecular "quantum dot"-like behavior. The orbitals in the highest subband of the highest VB are essentially the same as that in Fig. 8. The degree of localization can be judged from the dispersion (1.1 eV) which is about the same as that of the bands in quartz.[24] The orbitals around the bottom of the CB are of s^* type, while at $\bar{\Gamma}$ it is a π-bonded combination of $3p_x$–$3p_y$ hybrids around the ring, with Si–O–Si antibonds between the rings.

The main evidence for Si_6-rings acting as chromophores in siloxene comes from chemical substitution experiments. Looking again at Fig. 3(c), one notes that each Si atom belonging to a Si_6-ring is bonded to one hydrogen atom. It is now possible by more or less complicated chemical reactions to replace one hydrogen atom after the other with different monovalent radicals such as Cl, OH, NH_2, OCH_3, etc. Depending on the electronegativity of the radicals, this substitution has pronounced effects on the optical properties (absorption and fluorescence) of the resulting siloxene derivatives. In particular, for a given radical, the substitution occurs in six distinct steps.[16,25] As a specific example, we have modeled the effect of OH sub-

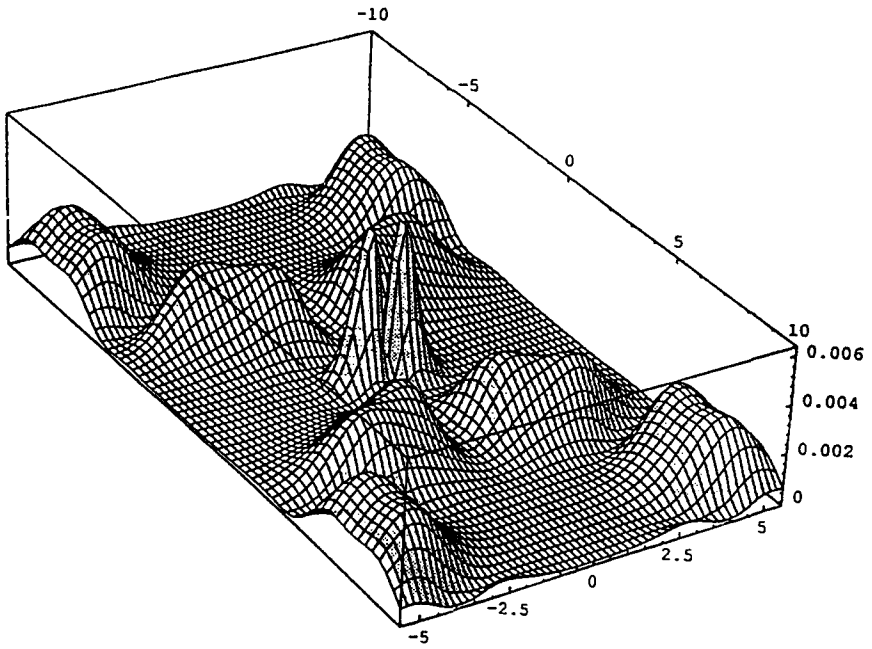

Fig. 8. Contour plot of the probability distributions for the highest valence band state of siloxene in the Si_6 ring modification. The sharp peaks at the center are due to 2*p*-orbitals of the oxygen bridge joining the two Si-rings. The positions of Si atoms are at the density minima.

stitution on the electronic properties of siloxene in the Si_6-ring modification. The different possible chemical compositions in this case are $[Si_6H_{6-x}(OH)_xO_3]_n$ with $0 \leq x \leq 6$ (the configuration $x = 0$ corresponds to the situation described in Figs. 7(c)). With increasing degree of H vs. OH substitution, we obtain from our calculations a significant decrease of both the direct and the indirect optical transition energies, which is in qualitative agreement with the available experimental evidence (N.B. no excitonic effects have been taken into account in the calculation). Substituting the H terminators with the more electronegative radicals OH will diminish the electron population in the bonding orbitals around the Si rings, weakening the bond and decreasing the bonding–antibonding splitting. As a result, both the direct and the indirect gap decreases. A comparison between theoretical and experimental optical transition energies is given in Table 1.

Soon after our results, further theoretical studies on siloxene have been reported[27,28] using the more sophisticated local density approximation (LDA) in supercell band structure calculation. Takeda and Shiraishi[27] have calculated the electronic structure of single planes for all three ideal siloxene modifications using a localized (minimal) basis set. The geometry was fixed using standard bond lengths and 180° bond angles for oxygen. The dispersion in the highest VB is remarkably similar to ours in all three cases (in Ref. 27, the point $\bar{K}$ is denoted as X

Table 1. Effect of H → OH substitution on the optical properties of $[Si_6H_{(6-x)}(OH)_xO_3]_n$, $0 \leq x \leq 6$. E($\bar{\Gamma}$) and E($\bar{K}$) denote direct optical gaps at different points of the Brillouin zone, E ($\bar{K} - \bar{\Gamma}$) is the calculated indirect gap for transitions between $\bar{K}$ and $\bar{\Gamma}$. Experimental luminescence data are taken from the work of Kautsky and Herzberg.[16]

x	$E(\bar{\Gamma})$/eV	$E(\bar{K})$/eV	$E(\bar{\Gamma} - \bar{K})$/eV	E_{lum}/eV
0	4.2	3.5	2.8	≥ 3.0
1	4.0	3.3	2.7	2.5
2	3.9	3.1	2.5	2.2
3	3.9	2.9	2.4	1.9
6	3.8	2.3	1.8	1.6

and the point $\bar{M}$ as S). For the plane modification, the lowest CB is also similar. The calculated gap is direct, its width is 1.66 eV. This is to be compared to our value of 2.7 eV. (Note that the density functional theory, without self-energy correction, underestimates the gap. Takeda and Shiraishi report a gap of 0.7 eV for bulk silicon.[24]) The CB of the chain- and ring-modifications appears to be significantly different from ours. The calculated band gap in the chain-modification is indirect, $E(\bar{M} - \bar{K}) \approx 3.2$ eV. The ring-modification is again calculated to have a direct gap at $\bar{\Gamma}$. The first transition of 0.63 eV is symmetry forbidden, while the second strong transition has an energy of ≈ 1.5 eV. Van de Walle and Northrup[28] have calculated the electronic structure of the plane modification, both for an isolated plane and for a three-dimensionally periodic lattice. The wave functions have been expanded on a large plane wave basis. The geometry has been optimized: the equilibrium bondlengths and angles are found to be about the same as in our calculation (with somewhat longer Si–H bonds). The interplanar distance is 5.3 Å. The heat of formation relative to crystalline Si and water is calculated to be −0.9 eV/unit, which (using the experimental heat of formation for water) gives −3.4 eV as the heat of formation from the standard state of the constituents. This is somewhat more than our AM1 value (−2.9 eV), probably due to the inclusion of long-range interactions. The reported band structure refers to the three-dimensionally periodic stack of planes, and is very similar to the one published by Takeda and Shiraishi, and by us. The authors note, that the interaction of the planes does not significantly change the shape of the bands; it causes only a 0.3 eV decrease in the gap. The calculated gap is 0.8 eV. Adding 0.3 eV to it gives 1.1 eV, which is still much lower than the one obtained by Takeda and Shiraishi.[27] This is probably due to the difference in the choice of the basis set. Van de Walle and Northrup also calculated the self-energy correction for the planar polysilane, $[HSi_2H]_n$. Based on the similarity of the band edge states between $[HSi_2H]_n$ and $[HSi_2(OH)]_{3n}$, they used the same correction, 0.9 eV, for the gap of the latter. This leads to an estimated first transition of 1.7 ± 0.3 eV for a three-dimensionally periodic, infinite siloxene crystal in the plane-modification.

5. Experimental Results on the Optical Properties of Siloxene

The large spectral range that can be covered by the strong photoluminescence of siloxene and siloxene derivatives is summarized in Fig. 9. Shown is the blue luminescence observed for Kautsky siloxene with a peak around 500 nm, the green-to-yellow luminescence of Wöhler-siloxene, and the red luminescence of siloxene after annealing at 400° C in ambient atmosphere. In the annealed state, the luminescence of siloxene resembles very much the strong visible luminescence observed in anodically etched porous silicon.[3,4] Annealing of siloxene at temperatures above 200° C leads to a change of the luminescence color from blue to green to red. The influence of annealing temperature on various structural and optical properties of Kautsky siloxene is summarized in Table 2. The main observations are

(i) The Si-planes of the siloxene modification in Fig. 3(a) are quickly destroyed, as evidenced by the disappearance of the X-ray diffraction peak at $2\Theta \approx 14°$ (cf. Fig. 4). Simultaneously, the IR peak at $520\,cm^{-1}$ disappears.

(ii) Above 200° C, hydrogen starts to evolve, accompanied by an increase of the ESR spin density associated with Si dangling bonds. The intensity of the Si–H stretching frequency at $2100\,cm^{-1}$ diminishes, and sidebands at around $2250\,cm^{-1}$ appear.

(iii) The optical gap (defined as the energy at which the absorption reaches 50%) decreases from about 2.8 eV to 1.9 eV, which can be seen as a color change from gray to red and eventually black.

(iv) A second luminescence band centered at about 700 nm (1.8 eV) slowly develops and reaches a pronounced intensity maximum after annealing at 400° C for

Table 2. Changes in the structural and optical properties of Kautsky siloxene as a function of isochronal annealing in air, I(X) denotes the relative intensity of the X-ray diffraction peak corresponding to the interplanar distance, I(IR) is the intensities of the infrared absorption peaks at the specified wavenumbers, and I(lum) is the normalized luminescence intensity at 700 nm. N_s is the ESR spin density and E_{gap} denotes the optical gap (absorptance = 0.5).

T_A(° C)	I(X) $d = 6.3$ Å	I(IR) $520\,nm^{-1}$	I(IR) $2100\,cm^{-1}$	N_s (cm^{-3})	I(lum) 700 nm	E_{gap} (eV)	Color
as-prep.	1	1	1	1.10^{16}	1	2.75	gray
100	—	0.5	0.9	1.10^{16}	5	2.8	gray
200	0.5*	0.3	0.8	1.10^{16}	5	2.9	gray
300	0*	0.1	0.7	1.10^{17}	10	2.8	gray
400	0	0	0.1	2.10^{18}	200	2.2	red
500	—	0	0	2.10^{19}	—	1.95	dark brown
600	—	—	—	2.10^{19}	—	1.9	black

*From Ubara *et al.* [17] for annealing in vacuum.

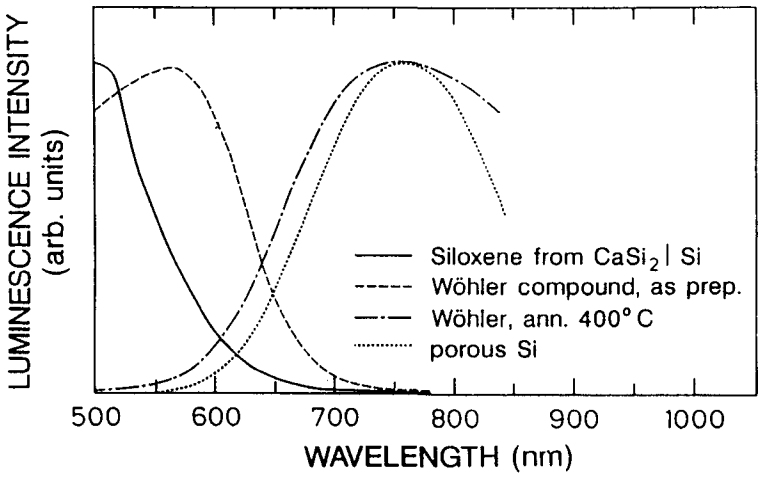

Fig. 9. Photoluminescence spectra of siloxene prepared as a thin layer on crystalline silicon as well as of Wöhler siloxene in the as-prepared state and after annealing at 400° C. The luminescence spectrum of anodically etched porous Si is shown for comparison. All spectra were taken at 300 K.

10 min. (see Fig. 9). The intensity of this luminescence is about a factor of 10 smaller than the green luminescence of as-prepared siloxene, which may be partly due to the larger defect density. Annealing at temperatures above 400° C leads to a complete disappearance of the luminescence.

Photoluminescence, photoluminescence-excitation and optical absorption spectra for Wöhler siloxene are shown in Fig. 10. At room temperature, as-deposited Wöhler siloxene has its luminescence maximum at $\hbar\omega \approx 2.35$ eV and is most efficiently excited in a narrow peak centered around 2.6 eV. For excitation below 2.5 eV, the luminescence peak follows the excitation energy with a Stoke shift of about 0.25 eV. A similar behavior has been reported for siloxene at 4.2 K by Hirabayashi *et al.*[29] The peak in the excitation spectrum of heat-treated siloxene samples is at higher energies than in the as-deposited sample. This is shown in Fig. 11. The excitation spectrum of samples luminescing at ≈ 1.65 eV (750 nm) show a shoulder around 3 eV with additional structures above 3.5 eV.

Further information about optical transitions beyond the sharp excitonic peak around 2.5 eV in the excitation spectrum of Wöhler siloxene can be obtained from energy dependent ellipsometry. In Fig. 12, we compare Wöhler siloxene with microcrystalline silicon. Starting from the direct gap siloxene exhibits a monotonically increasing absorption with a step at ≈ 4.4 eV. In crystalline Si, the absorption maximum at the same energy is due to direct transitions at the X-point. Note that the maximum absorption coefficient in siloxene is about a factor of three lower than in bulk silicon, as expected from the smaller Si–Si bond density in siloxene.

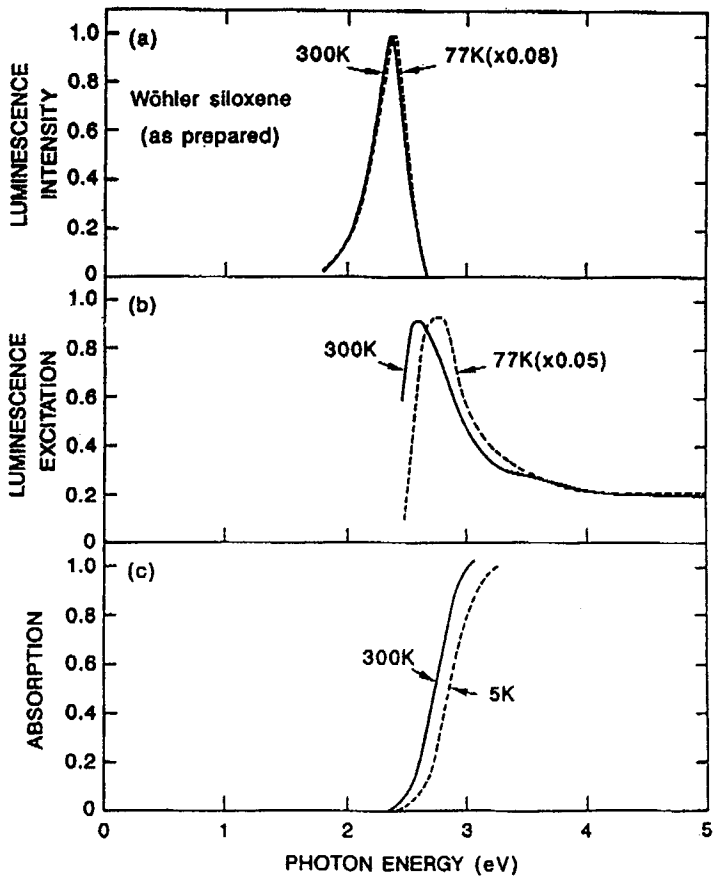

Fig. 10. The normalized photoluminescence, photoluminescence-excitation, and optical absorption spectra of as-prepared Wöhler siloxene at 300 K (solid lines) and at low temperature (dashed lines).

Figure 13 shows luminescence decays after pulse excitation with a blue laser line (λ_{ex} = 458 nm). The measurements were done at 300 K. The transients are not simple exponentials, but consist of a fast initial decay followed by a slower tail. Initial decay times are of the order of 1 μsec or less, whereas the slower decay extends to time constants of approximately 10 μsec, depending on the exact photoluminescence wavelength which is being monitored. It is interesting to compare the results in Fig. 13 to earlier time-resolved luminescence data at 4.2 K reported in Ref. 29. There, almost the same behavior was observed, with an initial decay time constant of $\approx$ 10 nsec and a long transient extending to about 10 μsec. This suggests that there is only a weak temperature dependence of the radiative lifetime in as-prepared siloxene.

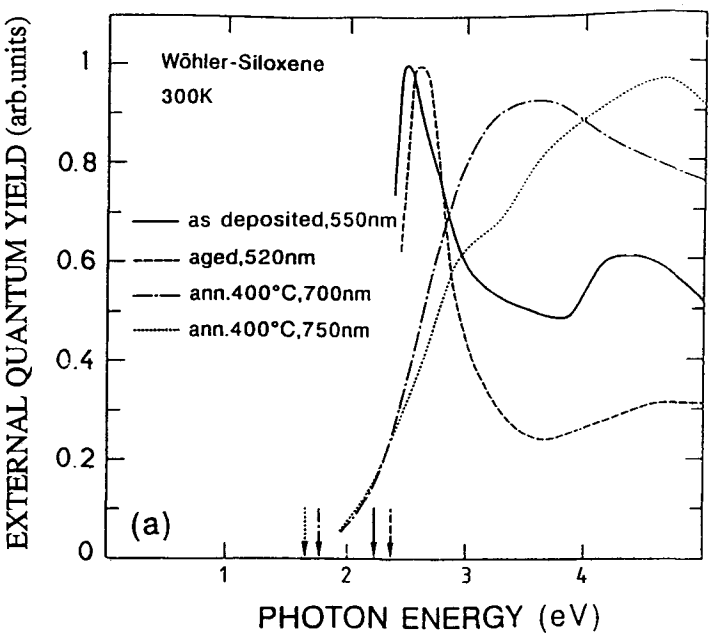

Fig. 11. Luminescence excitation spectra of Wöhler siloxene at 300 K. Arrows denote the energy at which the luminescence was monitored.

In Fig. 14 we present optically detected magnetic resonance (ODMR) spectra for Kautsky siloxene annealed at 400° C. The sample showed red luminescence at about 600 nm and had an ESR spin density of $2.5.10^{18}$ spins/g. The g-value was 2.0050, indicating silicon dangling bond defects as the structural origin of the spins. At 100 K, the same spin signal is also observed in the ODMR as a quenching signal (decrease of the luminescence intensity at spin resonance). This demonstrates that the dangling bond defects act as nonradiative recombination centers in annealed siloxene.

An effect which is commonly observed in both porous silicon and in siloxene is a pronounced luminescence fatigue during long excitation with visible or UV light. Several examples are shown in Fig. 15, where excitation occurred at 300 K with a wavelength of 458 nm in air. The luminescence monitored at 520 nm decreases irreversibly by two orders of magnitude in about 2 hours. The decay follows a simple bimolecular reaction rate and is proportional to $1/t$ for long times. At the same time the form of the infrared absorption spectra changes as shown in Fig. 5, relating the luminescence decrease to a destruction of the siloxene Si-planes. Hirabayashi *et al.* observed a similar fatigue effect also at 4.2 K. They report that the fatigue is only partly reversible in as-prepared siloxene, whereas a sample annealed at 350° C with a red luminescence exhibits a completely reversible luminescence fatigue[30]: after quenching the luminescence by prolonged illumination at 4.2 K to about one-tenth

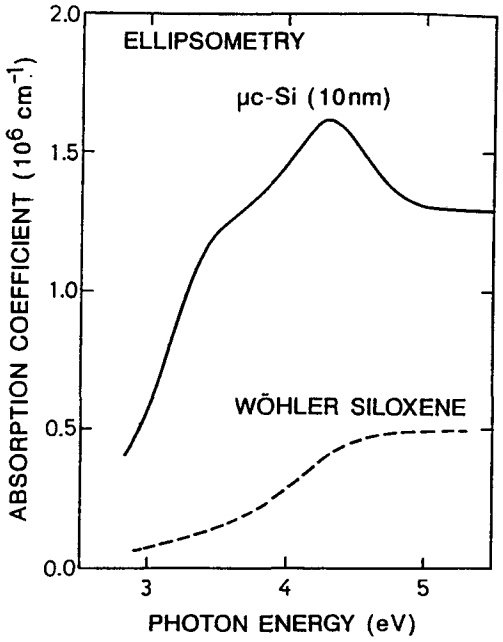

Fig. 12. Absorption coefficient of Wöhler siloxene obtained from spectroscopic ellipsometry. Data for microcrystalline Si are shown for comparison.

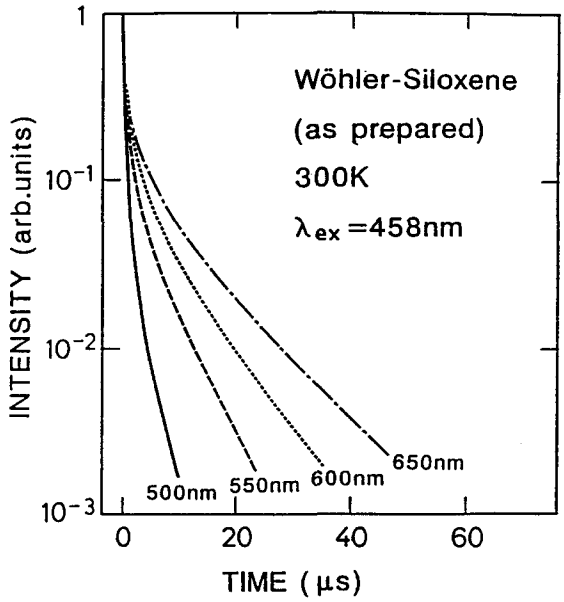

Fig. 13. Luminescence decay in as-prepared siloxene following pulse excitation with a 458 nm laser at 300 K. Different transients correspond to different wavelengths at which the luminescence was measured.

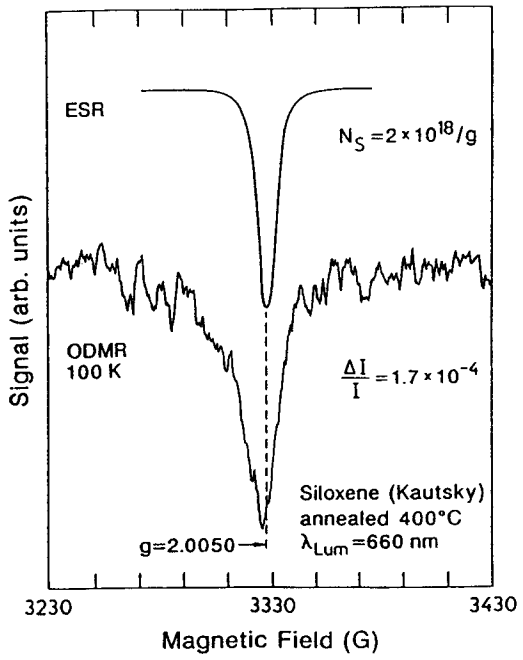

Fig. 14. Electron spin resonance (ESR) and optically detected magnetic resonance spectra (ODMR) of Kautsky siloxene annealed at 400° C with a luminescence at 660 nm.

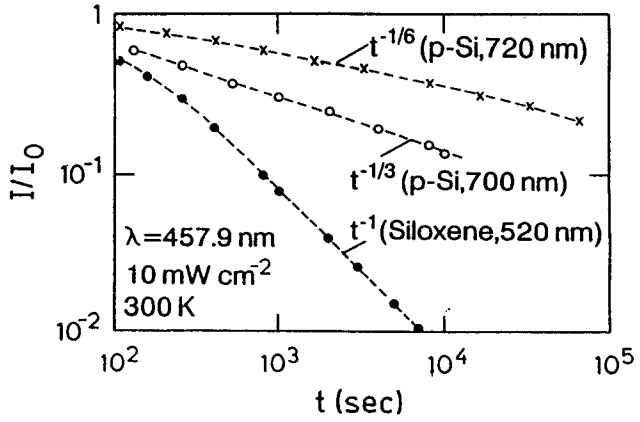

Fig. 15. Normalized decay of the photoluminescence intensity in siloxene and porous Si during long illumination in air. Illumination was done at room-temperature with an intensity of 10 mW/cm^2 at 458 nm.

of the initial intensity, annealing at room-temperature produces a complete recovery of the luminescence. This behavior is reminiscent of the luminescence fatigue in hydrogenated amorphous silicon[31] and certainly deserves a detailed investigation in the future.

7. The Origin of the Bright Luminescence in Siloxene

Based on the experimental results and the theoretical calculations outlined in the preceding section, a consistent explanation can be given for the optical properties of siloxene. According to the X-ray and infrared results, as-prepared Kautsky-siloxene contains dominantly the plane modification of stoichiometric siloxene /$[HSi_2(OH)]_{3n}$/. The direct gap predicted at $\approx$ 2.7 eV by our quantum chemical calculations for this modification is consistent with the observed optical gap and the blue luminescence. If Wöhler siloxene is a mixture of stoichiometric and substituted /$[HSi_2(OH)]_{xn}$+$[(OH)Si_2(OH)]_{(3-x)n}$/ siloxene, its electronic structure should be similar to the former, with lower transition energies. This is, in fact, the case: the excitonic peak in the excitation spectrum is at 2.5 eV, and the luminescence is green. The absorption spectrum of Wöhler siloxene shows a step at around 4.4 eV, which can be assigned to direct transitions between states along $\bar{\Sigma}$ found above 4.2 eV in our calculation for the unsubstituted plane-modification. (The same transition is calculated to be about 4.3 in Ref. 27 and 3.8 eV in Ref. 28.)

Upon low temperature annealing, the transformation of the metastable plane-modification begins. The first direct transitions calculated by our quantum chemical method for the modifications with oxygen inserted into the Si plane are higher than for the plane modification. This is consistent with the increase in the optical gap (Table 2).

For higher temperatures (around 400° C), H $\rightarrow$ OH substitutions occur more frequently and the oxygen insertion becomes complete. Both the gap and the luminescence is strongly red-shifted, and the luminescence intensity increases. This can be explained assuming the dominance of substituted rings and using the calculational results in Table 1 and Figs. 7(c) and 8. According to our calculation, efficient excitation of electron-hole pairs in the ring modification can be achieved at the energies of the two lowest direct transitions, which are expected below 2.9 eV and 3.9 eV, respectively, for siloxene derivatives luminescing in the red (Table 1). This compares well to the experimental excitation spectrum (Fig. 11). Radiative band-to-band recombination, on the other hand, occurs with lowest transition energy corresponding to the indirect gap between σ_{ring} ($\bar{\Gamma}$) and $s^*(\bar{K})$. Thus, the large apparent Stokes shifts can be explained by the thermalization of the carriers from the direct gap to the indirect gap. The difference between the calculated indirect transitions and the observed luminescence energies (Table 1) is in agreement with the observed Stokes shift of 0.25 eV. The indirect gap also explains the long radiative lifetimes. Figure 8 explains the exceptional strength of the luminescence, despite of the indirect gap. An exciton may get trapped in one of the rings, and due to the quantum-dot like nature of the orbitals, the transition may occur locally without consideration to linear momentum selection rules. The localization of the exciton gives rise to the Stokes shift.

The red luminescence of siloxene, therefore, can be attributed to the Si_6 rings isolated in the plane by the ordered insertion of oxygen atoms and having out-of-

plane bond-terminators which diminish the electron density in the ring. The latter role can, in fact be played by the Si–O–Si linkages developing between the planes upon annealing. Our preliminary results show that the electronic structure of two siloxene planes in the ring-modification but interconnected with Si–O–Si bridges is very similar to that of a single plane in the ring-modification with 3 hydrogens substituted by OH groups.

The ordered insertion of oxygen atoms in the ideal ring-modification has an effect on the infrared vibrations as well. Our AM1 calculation[18] (reproducing the phonon mode of the plane-modification at $478\,cm^{-1}$ and that of the ring at $469\,cm^{-1}$) predicts a double peak for the in-plane Si–O–Si stretching vibrations around 1050 and $1110\,cm^{-1}$, respectively. Figure 5 shows two structures to develop at about 1070 and $1160\,cm^{-1}$ in the absorption spectrum upon heat treatment. For high temperature annealing (which also destroys luminescence) this structure dissolves into a broad peak around $1050\,cm^{-1}$, typical of Si–O–Si vibrations in amorphous SiO_2.

8. Summary

We have presented a brief review of structural and optical properties of siloxene and related chemical derivatives. The basic structural units of stoichiometric siloxene are quasi-two-dimensional silicon planes, quasi-one-dimensional Si-chains, or quasi-one-dimensional sixfold Si rings isolated by oxygen and terminated by H and OH radicals. Preparation of siloxene occurs via a topochemical reaction starting from $CaSi_2$. Siloxene shows a strong luminescence which can be tuned over the entire visible range. The optical gap in as-prepared Kautsky-siloxene is around 2.7 eV. The green luminescence of Wöhler siloxene is most efficiently excited in a narrow band around 2.5 eV and exhibits decay times between 1 and $10\,\mu sec$. Strong absorption ($\alpha = 5 \cdot 10\,cm^{-1}$) in siloxene occurs for photon energies above 4.3 eV. The color of the luminescence can be changed to red either by chemical substitution of hydrogen or by simple annealing in air at 400° C. Upon annealing the optical gap diminishes to 2.2 eV, and the luminescence peak shifts to 1.6 eV, nevertheless, the Stokes shift is only about 0.25 eV. ODMR measurements indicate that dangling bond defects in annealed siloxene act as nonradiative recombination centers. Quantum chemical calculations indicate band structures for the three different modifications which are completely different from those of bulk crystalline Si and explain the interesting optical properties of siloxene in terms of carrier confinement into low-dimensional silicon structures due to the presence of oxygen atoms (chemical quantum confinement).

Acknowledgments

We thank M. Cardona and H.-J. Queisser for their support and helpful comments. We especially thank A. Breitschwerdt for the IR measurements and V. Lehmann

and J. Köhler for performing the X-ray diffraction studies. The support of the grant ESPRIT-7839 is gratefully acknowledged.

References

1. L. T. Canham, *Appl. Phys. Lett.* **57**, 1046 (1990).
2. V. Lehmann and U. Gösele, *Appl. Phys. Lett.* **58**, 856 (1991).
3. M. S. Brandt, H. D. Fuchs, M. Stutzmann, J. Weber and M. Cardona, *Solid State Commun.* **81**, 307 (1992).
4. M. Stutzmann, J. Weber, M. S. Brandt, H. D. Fuchs, M. Rosenbauer, P. Deák, A. Höpner and A. Breitschwerdt, *Adv. Solid State Phys.* **32**, 179 (1992).
5. P. McCord, Y. Shueh-Lin and A. J. Bard, *Science* **257**, 68 (1992).
6. E. A. Meulenkamp, P. M. M. C. Bressers and J. J. Kelly, *Appl. Surf. Sci.* **64**, 283 (1993).
7. M. A. Tischler and R. T. Collins, *Sol. State Commun.* **84**, 819 (1992).
8. W. Wang, H. C. Cheng and X. L. Zheng, *Mater. Lett.* **14**, 343 (1992).
9. F. Wöhler, *Lieb. Ann.* **127**, 257 (1963).
10. J. F. Morar and M. Wittner, *J. Vac. Sci. Technol.* **A6**, 1340 (1988).
11. H. Kautsky, *Z. Anorg. Chem.* **117**, 209 (1921).
12. A. Weiss, G. Beil and H. Meyer, *Z. Naturforschung* **35b**, 25 (1980).
13. M. S. Brandt, A. Breitschwerdt, H. D. Fuchs, A. Höpner, M. Rosenbauer, M. Stutzmann and J. Weber, *Appl. Phys.* **A54**, 567 (1992).
14. N. Matsumoto, K. Takeda, H. Teramae and M. Fujino, *Adv. in Chem.*, Vol. 224 (Amer. Chem. Soc., Washington, 1990), p. 515.
15. H. Kautsky, W. Vogell and F. Oeters, *Z. Naturforsch* **10B**, 597 (1955).
16. H. Kautsky and G. Herzberg, *Z. Anorg. Allg. Chem.* **139**, 135 (1924).
17. H. Ubara, T. Imura, A. Hiraki, I. Hirabayashi and K. Morigaki, *J. Non-Cryst. Solids* **59/60**, 641 (1983).
18. P. Deák, M. Rosenbauer, M. Stutzmann, J. Weber and M. S. Brandt, *Phys. Rev. Lett.* **69**, 2531 (1992).
19. P. Deák and L. C. Snyder, *Phys. Rev.* **B45**, 11612 (1992).
20. P. Deák and L. C. Snyder, *Phys. Rev.* **B36**, 9619 (1987).
21. H. Franz, A. Nikolov, T. Muschik, V. Petrova-Koch, V. Lehmann and J. Peisl, *"LESi II" Workshop on the Properties of Light Emitting Si*, Munnich, Germany, July 29–31, 1992.
22. P. Deák and J. Giber, *Phys. Lett.* **88A**, 237 (1982).
23. W. S. Verwoerd and K. Weimer, *J. Comput. Chem.* **12**, 417 (1991).
24. K. Takeda and K. Shiraishi, *Phys. Rev.* **B39**, 11028 (1989).
25. E. Hengge, *Chem. Ber.* **95**, 648 (1962).
26. G. Schott, *Z. Chem.* **3**, 41 (1963).
27. K. Takeda and K. Shiraishi, *Sol. State Commun.* **85**, 301 (1993).
28. C. G. Van de Walle and J. E. Northrup, *Phys. Rev. Lett.* **70**, 1116 (1993).
29. I. Hirabayashi, K. Morigaki and S. Yamanaka, *J. Non-Cryst. Solids* **59/60**, 645 (1983).
30. I. Hirabayashi, K. Morigaki and S. Yamanaka, *J. Phys. Soc. Japan* **52**, 671 (1983).
31. K. Morigaki, I. Hirabayashi, M. Nakayama, S. Nitta and K. Shimakawa, *Solid State Commun.* **33**, 851 (1980).